SCIENTIFIC REPORTS

OPEN

Tissue resident memory T cells in the human conjunctiva and immune signatures in human dry eye disease

Tanima Bose[1], Ryan Lee[2], Aihua Hou[2,3], Louis Tong[2,3,4,5] & K. George Chandy[1]

Non-recirculating resident memory (T_{RM}) and recirculating T cells mount vigorous immune responses to both self and foreign antigens in barrier tissues like the skin, lung and gastrointestinal tract. Using impression cytology followed by flow cytometry we identified two T_{RM} subsets and four recirculating T-subsets in the healthy human ocular surface. In dry eye disease, principal component analysis (PCA) revealed two clusters of patients with distinct T-cell signatures. Increased conjunctival central memory and naïve T cells characterized Cluster-1 patients, and increased CD8$^+$ T_{RM}s and CD4$^+$ recirculating memory T cells characterized Cluster-2 patients. Interestingly these T-cell signatures are associated with different clinical features: the first signature correlated with increased ocular redness, and the second with reduced tear break up times. These findings open the door to immune-based characterization of dry eye disease and T-subset specific immunotherapies to suppress T-subsets involved in disease. They may also help with patient stratification during clinical trials of immunomodulators.

Infections or antigenic challenge cause naïve T cells to differentiate into distinct memory T cell populations that are distinguished by their expression of the chemokine receptor CCR7 and the tyrosine phosphatase CD45 (T_{CM}: central memory T cells; T_{EM}: effector memory T cells: T_{EMRA}: effector memory T cells that have reacquired expression of CD45RA and lost CD45RO) (Fig. 1A)[1]. Each of these subsets can give rise to effector cells when challenged by their cognate antigen. In barrier tissues such as the skin, lung, gastrointestinal tract and genitourinary tract, T_{EM} and T_{EMRA} cells differentiate further into non-recirculating tissue resident memory T cells (T_{RM}), which persist for long periods in these tissues in the absence of antigens and provide immune protection[2–11]. The change from recirculating T_{EM}/T_{EMRA} cells to non-recirculating T_{RM} cells involves the acquisition of the type-C lectin CD69 and the integrin ($\alpha E\beta 7$) CD103 (Fig. 2A)[2–11]. Two subsets of T_{RM} cells have been described based on the expression of CD69 and CD103: CD69$^+$CD103$^-$ and CD69$^+$CD103$^+$ subsets[2–11]. Both T_{RM}-subsets are potent effectors, but CD69$^+$CD103$^+$ T_{RM}s exhibit limited proliferative capacity compared to CD69$^+$CD103$^-$ T_{RM}s[4,5]. The distribution of these T cell subsets has not been determined in the human ocular surface, a barrier tissue that protects sensitive internal structures responsible for vision[12].

The ocular surface consists of the cornea, the conjunctiva, the lacrimal gland and the lacrimal drainage system, and meibomian glands. The mucosa covering the avascular corneal surface at the visual axis contains mainly myeloid and dendritic cells, while the conjunctiva over the remainder of the ocular surface also contains lymphatics, diffuse and aggregated lymphocytes[13,14]. While T cell subsets have been described in the conjunctiva[13], the relative proportions of T_{RM} and recirculating T cells at this barrier surface have not been studied in humans or animal models. Such information could provide insights into ocular surface inflammation.

The most common and prominent manifestation of ocular surface inflammation is dry eye disease (DED). DED is a heterogeneous group of diseases, with overlapping but distinct clinical features. Symptoms of discomfort and visual disturbance as a result of tear instability, increased osmolarity of the tear film, and inflammation of the

---

[1]Laboratory of Molecular Physiology, Infection and Immunity Theme, Lee Kong Chian School of Medicine, Nanyang Technological University, 59 Nanyang Drive, 636921, Singapore. [2]Singapore Eye Research Institute, 20 College Road, 169856, Singapore. [3]Duke-NUS Medical School, 8 College Road, 169857, Singapore. [4]Singapore National Eye Center, 11, Third Hospital Avenue, 168751, Singapore. [5]Yong Loo Lin School of Medicine, 1E Kent Ridge Road Level 7, NUHS Tower Block, 119228, Singapore. Correspondence and requests for materials should be addressed to L.T. (email: louis.tong.h.t@singhealth.com.sg) or K.G.C. (email: gchandy@ntu.edu.sg)
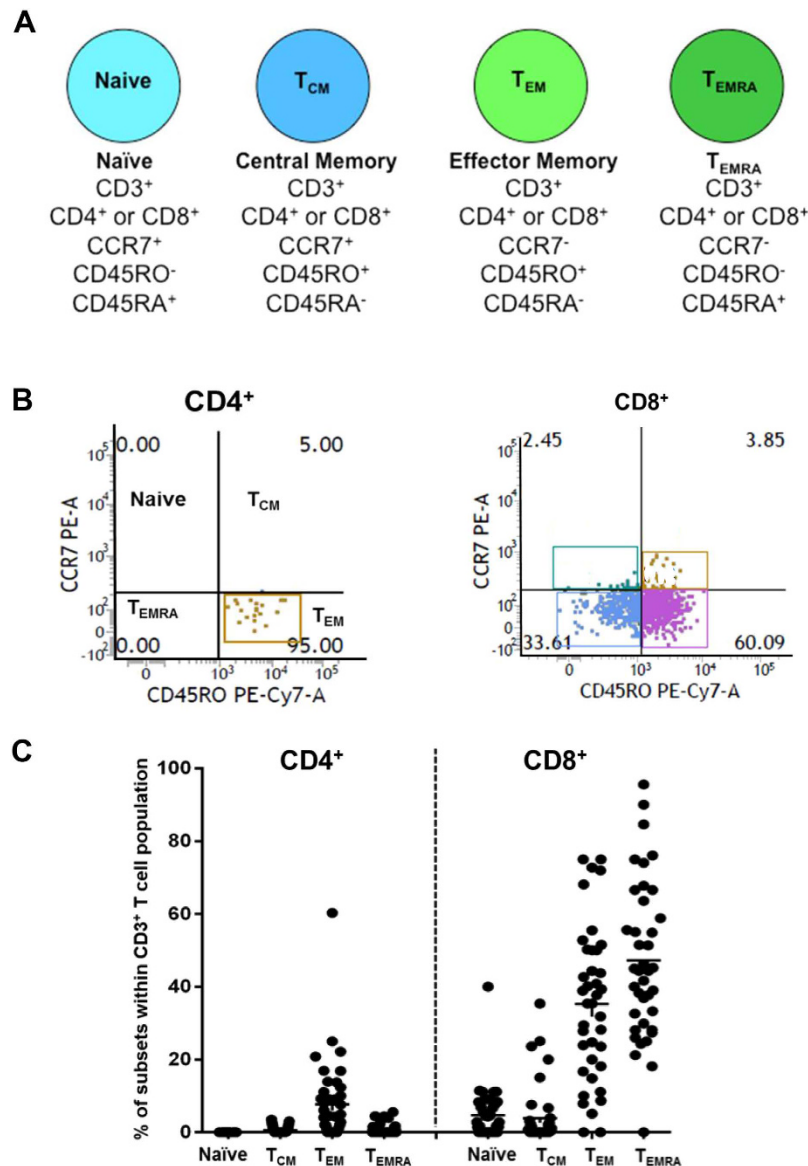
Figure 1. T-cell surface markers in normal ocular surface. (**A**) Cell surface markers for naïve, T_{CM}, T_{EM} and T_{EMRA} subsets used in our studies. (**B**) Flow cytometry showing proportion of naïve, T_{CM}, T_{EM} and T_{EMRA} subsets within CD4$^+$ and CD8$^+$ pools (*left and right panels*) in the nomal human conjunctiva. (**C**) Proportion of conjunctival naïve, T_{CM}, T_{EM} and T_{EMRA} subsets in CD4$^+$ and CD8$^+$ T cell pools expressed as a percentage of the total number of CD3$^+$ T cells in healthy human conjunctiva. Each data point represents a separate individual; mean ± SEM shown.

ocular surface characterize DED. The prevalence of DED increases with age, ranging from 5% in young adults to as much as 35% in people of 50 years and older[15–22]. It develops due to stress, autoimmune diseases (rheumatoid arthritis, systemic lupus erythematosus, Sjogren's syndrome), chemical injury, blepharitis, infections, meibomian gland dysfunction and allergies, and more devastating conditions such as Steven Johnson syndrome and graft-versus-host disease[15–22].

Many reports document the pathogenic role of T cells in animal models of DED[23,24]. The disease can be induced in animal models by the transfer of pathogenic T cells[25]. Animals with defects in regulatory T cells exhibit more severe DED[26,27]. The importance of T cells in human DED is underscored by the efficacy of cyclosporine, a T cell immunosuppressant that is a cornerstone of DED therapy[28–30]. Here, we use impression cytology and flow cytometry to determine the distribution of T_{RM} and recirculating T cell subsets at the ocular surface in healthy humans and in patients with dry eye disease. We demonstrate that the human ocular surface is protected by two subsets of T_{RM} cells and four subsets of recirculating T cells. We describe two immunological signatures in DED patients along with distinguishing clinical profiles. Our results raise the possibility of using the immune signatures and related clinical findings to stratify patients during clinical trials of immunomodulators. It also
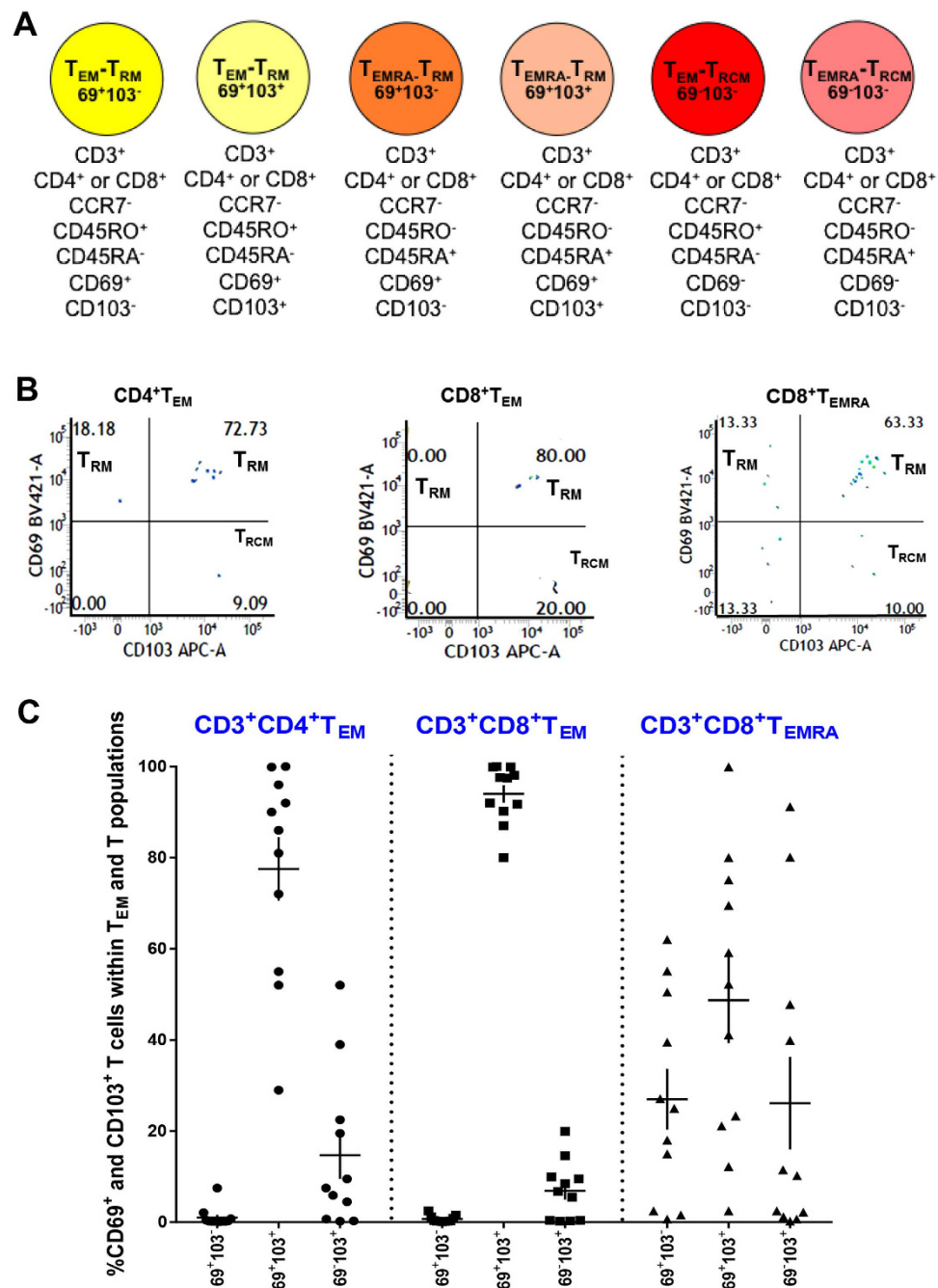
Figure 2. Tissue resident memory T cells predominate in the human ocular surface. (**A**) Cell surface markers for T_{RM} and T_{RCM} subsets used in our studies. (**B**) Flow cytometry showing proportion of $CD69^+CD103^-T_{RM}$, $CD69^+CD103^+$ T_{RM} and T_{RCM} in $CD4^+$ T_{EM}, $CD8^+$ T_{EM} and $CD8^+$ T_{EMRA} subsets. (**C**) Proportion of conjunctival T_{RM}s ($CD69^+CD103^-$, $CD69^+CD103^+$), T_{RCM} ($CD69^-CD103^+$) subsets within T_{EM} and T_{EMRA} pools in healthy controls. The different T_{RM} populations in each T_{EM}/T_{EMRA} pool do not add up to 100% because we did not include $CD69^-CD103^-$ T cells in the figure. Each data point represents a separate individual; mean $\pm$ SEM shown.

suggests the feasibility of developing an immune-based classification of DED and could lead to novel immuno-therapies that target specific immune signatures to complement current broadly immunosuppressive therapies.

Results

CD8$^+$ tissue resident memory T cells predominate in the normal human ocular surface.

We selected 39 healthy controls based on the absence of history of DED symptoms in the preceding 3 weeks determined by the SPEED (Standard Patient Evaluation of Eye Dryness) questionnaire, and normal scores on the Schirmer's Test and non-invasive tear breakup time (NI-TBUT) (Supplementary Table S1,

Supplementary Figure S1). Four impressions were obtained per individual, two impressions from each eye. Cells were isolated from the membrane and flow cytometry used to analyse T cell subsets (Fig. 1A). CD3$^+$ T cells were gated out and live AAD$^-$ cells selected. The total number of CD3$^+$ T cells obtained from each patient varied from ~300–1800. We determined the proportions of CD4$^+$ and CD8$^+$ T cells within the CD3$^+$ pool (Fig. 1B). We then measured the proportions of naïve, T$_{CM}$, T$_{EM}$ and T$_{EMRA}$ T cells within the CD4$^+$ and CD8$^+$ pools. CD8$^+$ T cells accounted for ~90% of CD3$^+$ T cells in the normal conjunctiva (Fig. 1C). Of CD8$^+$ T cells, ~80% were CCR7$^-$ T$_{EM}$ and T$_{EMRA}$ cells, and a minority were CCR7$^+$ naïve T and T$_{CM}$ cells (Fig. 1C). Only 10% were CD4$^+$ T cells and these were almost entirely T$_{EM}$ cells (Fig. 1C). Our results are consistent with an earlier study, which reported a preponderance of CD8$^+$ T$_{EM}$ cells in the ocular surfaces of a cohort of human volunteers in the UK[13].

We next measured the proportion of the two non-recirculating resident memory T$_{RM}$ subsets (CD69$^+$CD103$^-$, CD69$^+$CD103$^+$) within the cell populations above (Fig. 2A). A third subset (T$_{RCM}$) expresses CD103 but lacks CD69 (Fig. 2A). In rodents, this subset has been reported to be recirculating memory T cells that migrate from epithelial tissues via draining lymph nodes and the circulation to distant epithelial sites of inflammation[31]. We used coordinate analysis of CD69 and CD103 expression to quantify all three memory subsets within the CD8$^+$ and CD4$^+$ T$_{EM}$/T$_{EMRA}$ pools in conjunctivas of 13 healthy controls. Representative FACS profiles are shown in Fig. 2B. In both CD8$^+$ and CD4$^+$ T$_{EM}$/T$_{EMRA}$ subsets, CD69$^+$CD103$^+$ T$_{RM}$s accounted for 70–80%, and CD69$^+$CD103$^-$ T$_{RM}$s and T$_{RCM}$s each accounted for 5–10% (Fig. 2C). Since the chemokine receptors CCR6 and CXCR3 are necessary for T cell-mediated ocular surface inflammation in experimental DED[32], we measured T cell subsets expressing these receptors in our subjects. The majority of T cells were CXCR3$^+$CCR6$^-$, with CXCR3$^-$CCR6$^+$ and CXCR3$^+$CCR6$^+$ T cells being less abundant (Supplementary Figure S2). In summary, CD8$^+$ T$_{EM}$/T$_{EMRA}$ cells predominate in the human ocular surface. Of these the majority are CD69$^+$CD103$^+$ T$_{RM}$s. Four recirculating T cells subsets are also present: naïve, T$_{CM}$, T$_{EM}$/T$_{EMRA}$ and T$_{RCM}$s.

Two immune signatures in patients with dry eye disease.

We identified another 52 participants that satisfied our clinical criteria (see below) of having DED. Since DED is multifactorial, we were interested to know if the disease is heterogeneous in terms of conjunctival T cell composition. T cells in the conjunctiva of these 52 DED patients were therefore immunophenotyped to identify proportions of T subsets (naïve, T$_{CM}$, T$_{EM}$, T$_{EMRA}$, T$_{RM}$s, T$_{RCM}$) present during ocular surface inflammation. Patients with DED were selected based on presence of at least *two* of the following: complaints of dry eye symptoms >2 weeks duration determined by the SPEED questionnaire, and abnormal Schirmer's Test and/or NI-TBUT score. In our participants, DED was due to idiopathic causes (n = 30), Sjogren's syndrome (n = 5), graft-versus-host disease (n = 5), rheumatoid arthritis (n = 4), systemic lupus erythematosus (n = 2), glaucoma medications (n = 3), mixed connective tissue (n = 1), myelodysplasia (n = 1), and contact lens wear (n = 1) (Supplementary Tables S2 and S3). These patients were age-matched and gender-matched with the controls above (Supplementary Figure S1).

We performed principal component analysis of DED patients based on the proportion of different T cell subsets (CD4$^+$ and CD8$^+$ naïve, T$_{CM}$ and T$_{EM}$). Two clusters of patients were revealed when we plotted the first 2 principal components (Fig. 3A,B). Differences between these clusters were attributed largely to the first principal component (horizontal axis in Fig. 3B). We classified DED into two groups: 16 patients in Cluster-1 (red circle on right in Fig. 3A) and 36 patients in Cluster-2 (blue circle on left in Fig. 3A). Cluster-1 patients exhibited increased conjunctival CD4$^+$ and CD8$^+$ naïve and T$_{CM}$ cells and decreased CD4$^+$ and CD8$^+$ T$_{EM}$ and T$_{EMRA}$ cells compared to Cluster-2 patients (Fig. 4A). We refer to this T cell subset pattern in DED as *T-cell signature-1*. Cluster-2 patients had increased CD3$^+$ T$_{EM}$ and T$_{EMRA}$ cells compared to Cluster-1 patients (Fig. 4B). We refer to this T cell subset pattern as *T-cell signature-2*. The absolute numbers of T cells are shown in Supplementary Tables S4 and S5. In Cluster-1 patients CD3$^+$ T$_{CM}$ and naïve T cells (T$_{CM}$ = 588 ± 73; naïve = 180 ± 10) were higher than in Cluster-2 patients (T$_{CM}$ = 66 ± 12; naïve = 44 ± 12) (T$_{CM}$ = P < 0.0001; naïve = P < 0.01). In Cluster-2 patients, the absolute numbers of CD3$^+$ T$_{EM}$ and T$_{EMRA}$ cells (T$_{EM}$ = 853 ± 10; T$_{EMRA}$ = 617 ± 12) were higher than in Cluster-1 patients (T$_{EM}$ = 176 ± 10; T$_{EMRA}$ = 162 ± 12) (for both T$_{EM}$ and T$_{EMRA}$ subsets = P < 0.0001).

Comparison of T cell signatures in dry eye disease versus controls.

A logical next step is to determine differences between the two T cell signatures in DED with the controls evaluated in Figs 1 and 2. Using *t*-tests, we found that Cluster-1 patients had increased conjunctival CD4$^+$ and CD8$^+$ naïve and T$_{CM}$ cells, and decreased CD4$^+$ and CD8$^+$ T$_{EM}$ and T$_{EMRA}$ cells compared to controls (Fig. 4A). Cluster-2 patients had increased CD4$^+$CD69$^-$CD103$^+$ T$_{EM}$-T$_{RCM}$ and CD8$^+$CD69$^+$CD103$^+$ T$_{EMRA}$-T$_{RM}$, and decreased CD8$^+$CD69$^+$CD103$^-$ T$_{EMRA}$-T$_{RM}$ and CD8$^+$CD69$^-$CD103$^+$ T$_{EMRA}$-T$_{RCM}$ compared to controls (Fig. 4B). The absolute numbers of T cells are shown in Supplementary Tables S4 and S5. In Cluster-1 patients, the absolute numbers of CD3$^+$ T$_{CM}$ and naïve T cells (T$_{CM}$ = 588 ± 73; naïve = 180 ± 10) was higher than in controls (T$_{CM}$ = 73 ± 12; naïve = 58 ± 12) (for both T$_{CM}$ and naïve = P < 0.0001). In Cluster-2 patients, the absolute numbers of CD3$^+$ T$_{EM}$ and CD3$^+$ T$_{EMRA}$ patients (T$_{EM}$ = 853 ± 10; T$_{EMRA}$ = 617 ± 12) were similar to that in controls (T$_{EM}$ = 632 ± 12; T$_{EMRA}$ = 691 ± 12) (Supplementary Table S4). However, Cluster-2 patients had higher absolute numbers of CD8$^+$CD69$^+$CD103$^+$ T$_{EMRA}$-T$_{RM}$ (528 ± 8) and CD4$^+$CD69$^-$CD103$^+$T$_{EM}$-T$_{RCM}$ (101 ± 1) than controls (CD8$^+$CD69$^+$CD103$^+$ T$_{EMRA}$-T$_{RM}$ = 251 ± 6; CD4$^+$CD69$^-$CD103$^+$T$_{EM}$-T$_{RCM}$ = 9 ± 2) (CD8$^+$CD69$^+$CD103$^+$ T$_{EMRA}$-T$_{RM}$ = P < 0.0001; CD4$^+$CD69$^-$CD103$^+$T$_{EM}$-T$_{RCM}$ = P < 0.01). Cluster-2 patients had lower absolute numbers of CD8$^+$CD69$^+$CD103$^-$ T$_{EMRA}$-T$_{RM}$ (41 ± 2) and CD8$^+$CD69$^-$CD103$^+$ T$_{EMRA}$-T$_{RCM}$ (16 ± 2) compared to controls (CD8$^+$CD69$^+$CD103$^-$ T$_{EMRA}$-T$_{RM}$ = 132 ± 2; CD8$^+$CD69$^-$CD103$^+$ T$_{EMRA}$-T$_{RCM}$ = 146 ± 2) (CD8$^+$CD69$^+$CD103$^-$ T$_{EMRA}$-T$_{RM}$ = P < 0.05; CD8$^+$CD69$^-$CD103$^+$ T$_{EMRA}$-T$_{RCM}$ = P < 0.01) (Supplementary Table S4 and S5). These results indicate that the proportions of particular T$_{EM}$ and T$_{EMRA}$ subsets are altered in Cluster-2 patients, although the overall number of terminally differentiated CCR7$^-$ T cells in these patients is the same as in controls. We did not find any difference in the proportions of T cells expressing the chemokine receptors CXCR3 or CCR6 in
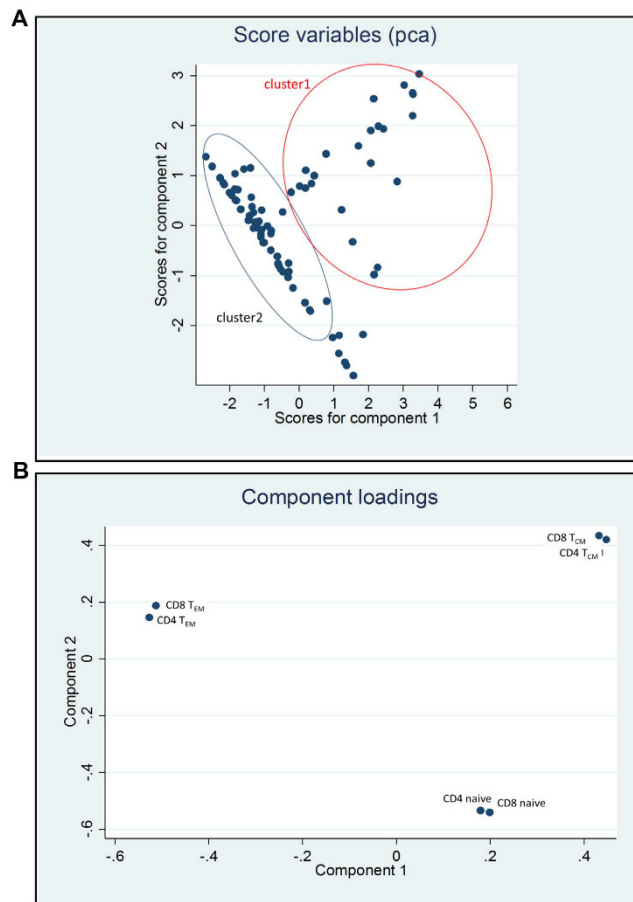
Figure 3. Principal Component Analysis reveals two T cell signatures in dry eye disease. (A) 2D Scatter diagram showing first 2 principal components. (**B**) Loading-plot showing the first principal component is largely determined by the ratio of T_{CM} to T_{EM}, a higher ratio will shift the point to the right of the horizontal axis, whereas a lower ratio will be represented on the left.

Cluster-1 or Cluster-2 patients compared to each other or to controls (data not shown). In summary, we identified two clusters of DED patients with distinct T cell immune signatures which are also significantly different from controls.

The two ocular T-cell signatures in dry eye patients correlate with different clinical features.

To understand the clinical implications of the two T cell signatures in DED, we examined whether Cluster-1 and Cluster-2 patients derived from principal component analysis demonstrated any differences in clinical phenotypes.

When *t-tests* were performed, we found that ocular redness (OR)[33] was significantly increased in Cluster-1 compared to Cluster-2 patients ($P < 0.001$) (Fig. 5A, Table 1). OR arises as a consequence of reactive dilation of conjunctival blood vessels (conjunctival hyperemia) and is a frequent response to diverse pathologic stimuli[33–35]. When all controls and patients were considered, we detected a positive linear correlation between OR scores and conjunctival CD4$^+$ T_{CM} (r = 0.5; $P < 0.0001$) and CD8$^+$ T_{CM} (r = 0.54; $P < 0.0001$), and an inverse correlation with conjunctival CD8$^+$ T_{EM} (r = −0.4; $P = 0.0057$) and T_{EMRA} cells (r = −0.5; $P = 0.002$) (Fig. 5B and Supplementary Fig. S3).

NI-TBUT assesses tear evaporation, spreading and elasticity of tears in DED. In Cluster-2 patients, shorter NI-TBUT is indicative of increased tear instability correlated with higher proportions of conjunctival CD4$^+$ T_{EM}-T_{RCM} (r = −0.4; $P < 0.0001$) and CD8$^+$ T_{EMRA}-T_{RM}s (r = −0.5; $P < 0.0001$) (Fig. 5D, Supplementary Figure S4).

When the data were re-analyzed only with patients with idiopathic DED, we found the same two clusters and associated clinical findings. This indicates that the differences in immune signatures are not likely to be due to differences in specific etiology of DED in the two clusters (specific etiologies provided in Supplementary Tables S2 and S3).

Dry eye disease is commonly classified into two clinical subtypes based on the Schirmer and NI-TBUT tests[21]. "Aqueous deficiency dry eye" is defined as a Schirmer test <5 mm, and "evaporative or tear deficiency DED" is defined as NI-TBUT <6 secs. In this study, 17% (9/52) of DED patients had pure aqueous deficiency DED (Fig. 6A), 37% (19/52) had pure evaporative/tear instability DED, 25% (13/52) had combined aqueous deficiency and evaporative DED, and 21% (11/52) did not qualify as aqueous or evaporative or mixed subtypes based on their average NI-TBUT and Schirmer values in the right and left eyes (Fig. 6A). We used Venn diagram analysis
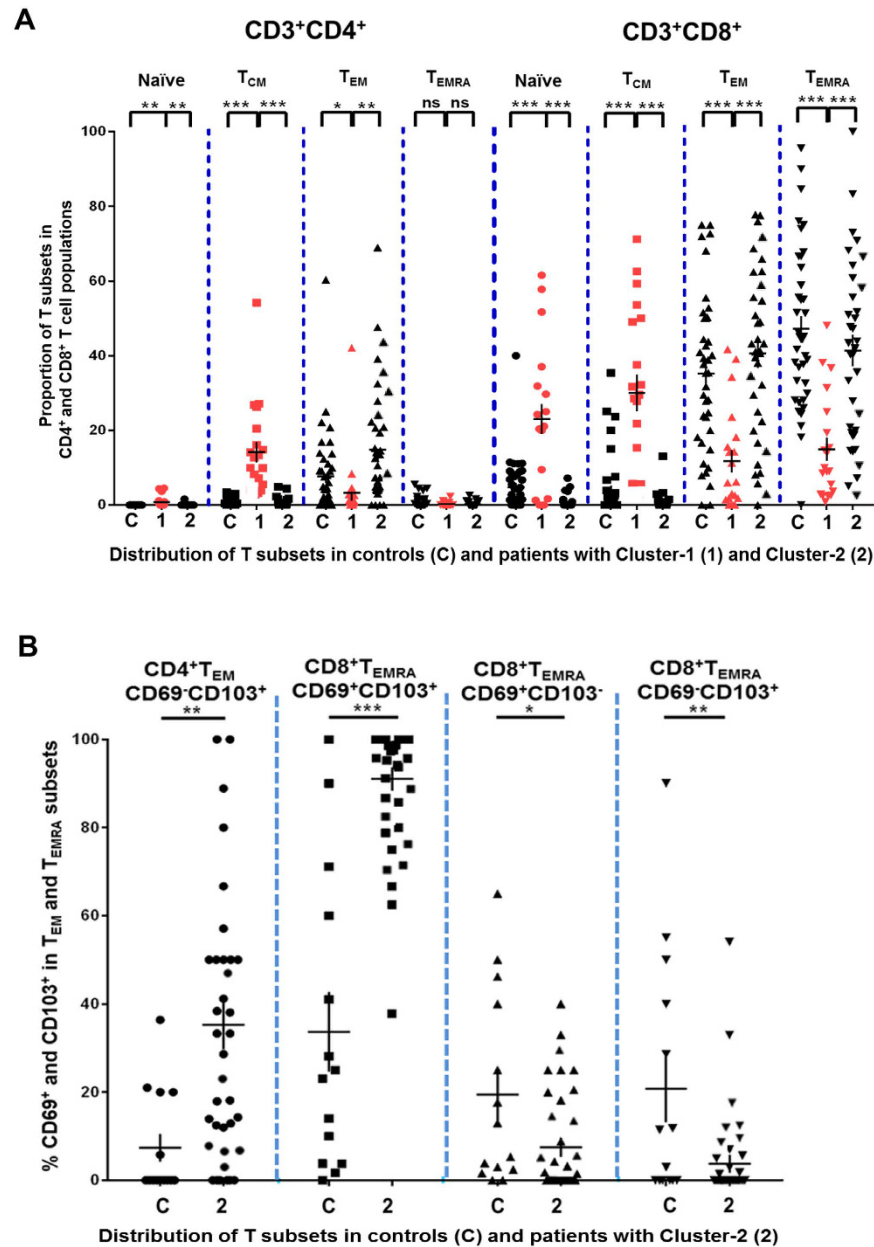
Figure 4. Two T cell signatures in dry eye disease. (**A**) Conjunctival CD4$^+$ and CD8$^+$ naïve, T$_{CM}$, T$_{EM}$ and T$_{EMRA}$ subsets in controls (C) and Cluster-1 patients (1) and Cluster-2 patients (2). Each data point represents a separate individual; mean ± SEM shown. (**B**) Conjunctival T$_{RM}$, T$_{RCM}$ subsets within CD4$^+$T$_{EM}$ and CD8$^+$ T$_{EMRA}$ pools in controls (C) and Cluster-2 patients (2). Each data point represents a separate individual; mean ± SEM shown.

to examine the overlap between Cluster-1 and Cluster-2 patients and these clinical subtypes of DED (Fig. 6A–C). There was a higher proportion of pure evaporative/tear instability sub-type patients in Cluster-2 (P = 0.027; Table 1, Fig. 6C). There were similar proportions of aqueous deficiency DED subtype and mixed cases in both clusters (Table 1, Fig. 6B and C). Our data provide additional non-redundant information about dry eye disease that might complement and facilitate patient stratification.

In summary, Table 1 shows that conjunctival redness (OR measured by an Oculus K5M)[33] was significantly higher in Cluster-1 compared to Cluster-2 patients (P < 0.001 in all comparisons). Cluster-2 had a higher proportion of females compared to Cluster-1 (Table 1). All other parameters were identical between the clusters (Table 1). Male gender was associated with a higher OR (P = 0.016), so gender could potentially confound the relationship between the T-cell clusters and OR. In a linear regression model with OR as a dependent variable and T-cell cluster and gender status as independent variables, T-cell clustering remained significant (P < 0.001) while gender was no longer significant (P = 0.5). Finally, the proportion of pure evaporative/tear instability sub-type patients was significantly higher in Cluster-2 (P = 0.027).
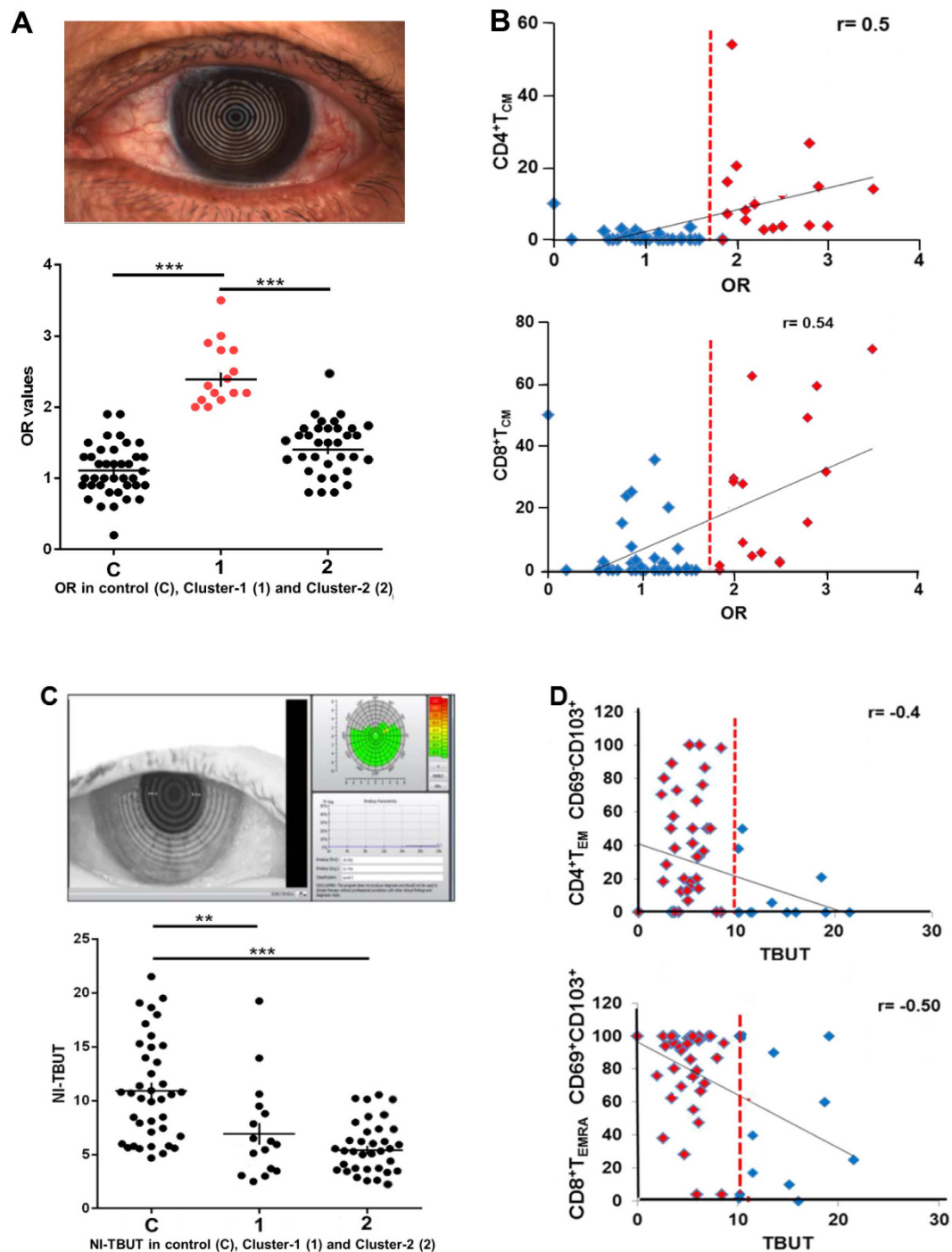
Figure 5. Correlation of two T cell signatures with clinical parameters. (**A**) *Upper panel*: ocular redness; *Lower panel*: Ocular redness (OR) scores in controls (C) Cluster-1 patients with T cell signature-1 (1) and Cluster-2 patients with T cell signature-2 (2). (**B**) OR scores show a positive correlation with $CD4^+$ T_{CM} and $CD8^+$ T_{CM}; controls (blue); Cluster-1 patients with T cell signature 1 (red); dotted red line indicates OR 1.9. Pearson's correlation coefficient was calculated for 55 subjects. Two-tailed $P < 0.0001$ for both the correlations. (**C**) *Upper panel*: Picture of ocular surface obtained with an Oculus Keratograph 5 M; *Lower panel*: NI-TBUT in controls (C) and Cluster-1 patients with immune signature-1 (1) and Cluster-2 patients (2). (**D**) NI-TBUT correlates with $CD4^+CD69^-CD103^+T_{EM}$-T_{RCM} and $CD8^+CD69^+CD103^+$ T_{EMRA}-T_{RM}; controls (blue); Cluster-2 patients with T cell signature-2 (red); dotted red line indicates NI-TBUT = 10 s. Pearson's correlation coefficient was calculated for 49 subjects. Two-tailed $P < 0.0001$.

Characteristic	Cluster 1 (n = 16)	Cluster 2 (n = 36)	P value[†††]
Age			
Mean ± SD	63.0 ± 15.1	56.0 ± 15.9	0.151
Median (min, max)	66.0 (27.0, 82.0)	58.6 (22.7, 90.7)	
Gender			
Women % (n)	44 (7/16)	86 (31/36)	<0.005[**]
Ocular redness[†]			
Mean ± SD	2.4 ± 0.6	1.5 ± 0.5	<0.001[***]
Median (min, max)	2.2 (1.4,3.5)	1.5 (0.8,2.9)	
NI-TBUT[††] (sec)			
Mean ± SD	7.8 ± 5.8	5.2 ± 2.5	0.120
Median (min, max)	6.2 (2.5, 25.0)	5.0 (2.6, 14.1)	
Schirmer I test (mm)			
Mean ± SD	8.4 ± 8.8	9.4 ± 11.4	0.749
Median (min, max)	4.5 (0.5, 31.0)	6.0 (0.0, 45.0)	
Subtype dry eye			
Aqueous deficient %(n)	19 (3/16)	17 (6/36)	1.000
Evaporative %(n)	13 (2/16)	47 (17/36)	0.027[*]
Mixed%(n)	38 (6/16)	19 (7/36)	0.184
Systemic disease			
Chronic GvHD (n)	3	3	0.357
Primary Sjogren syndrome (n)	0	5	0.308
Rheumatoid arthritis (n)	1	3	1.000
SLE (n)	0	3	0.544
Myelodysplasia (n)	1	0	0.308
Glaucoma (n)	2	2	0.578
Hypothyroidism (n)	1	0	0.308
Mixed connective tissue (n)	1	0	0.308
Ocular surgery			
(LASIK) (n)	0	1	1.000
Contact lens wear			
(n)	1	0	0.308
Idiopathic (n)	8	22	0.548

Table 1. Clinical characteristics of dry eye patients in Cluster-1 and Cluster-2. [†]Average temporal bulbar redness shown (measured by Oculus Keratograph 5 M). [††]Non-invasive tear break up time (measured by Oculus Keratograph 5 M). [†††]Two-tailed p value (either chi-square/Fisher exact test or *t-test*). *p < 0.05, **p < 0.01, ***p < 0.001.

Discussion

The ocular surface comprised of the cornea, conjunctiva, meibomian glands, and lacrimal gland and drainage system is a barrier tissue that protects the vision apparatus[12]. T lymphocytes have been described in the human and rodent conjunctiva[13], and ocular surface T cells play a critical pathogenic role in DED, the commonest clinical manifestation of ocular surface inflammation[22–30]. Here, we have used impression cytology and flow cytometry to characterize recirculating (naïve, T_{CM}, T_{EM}, T_{EMRA}, T_{RCM}) and non-recirculating (T_{RM}) T cell subsets (Figs 1A and 2A) in the healthy human ocular surface and in patients with DED.

In the healthy human ocular surface, CD8^{+} T cells are the majority subset, and they are predominantly terminally differentiated CD8^{+} T_{EM} and T_{EMRA} cells (Figs 1D and 7A). CD4^{+} T cells are a minority, but they too are mainly T_{EM} and T_{EMRA} cells (Figs 1D and 7A). CD8^{+} and CD4^{+} T_{EM} and T_{EMRA} cells are preponderantly non-recirculating T_{RM}s, the CD69^{+}CD103^{+} T_{RM} subset being most abundant (Figs 2A and 7A). We also detect recirculating CCR7^{+} naïve and T_{CM} cells, and recirculating CCR7^{−}CD69^{−}CD103^{−} T_{EM}, T_{EMRA} and T_{RCM} cells in the healthy human in ocular surface. This T cell-distribution is similar to that in the gastric lamina propria. In both the ocular surface and the stomach's lamina propria CD8^{+}CD69^{+}CD103^{+} T_{RM}s predominate and CD4^{+} T cells are a minority[10]. CD8^{+}CD69^{−}CD103^{+} T_{RCM} recirculating cells are also present in both tissues[10], but have not been reported in other barrier tissues such as the human skin, non-inflamed human lung, and intestinal and cervical mucosa. In the human dermis and non-inflamed lung CD4^{+}CD69^{+}CD103^{−} T_{RM}s predominate, while in the human epidermis, intestinal mucosa and cervical mucosa a mixture of CD4^{+} and CD8^{+} CD69^{+}CD103^{+} T_{RM} cells are present[2–11]. We do not yet understand the reasons for the similarity of the T cell profile in the human conjunctiva and other tissues.

Ocular surface inflammation in DED can arise from multiple etiologies including autoimmunity (Sjogren's syndrome, rheumatoid arthritis, systemic lupus erythematosus), blepharitis, and cicatrizing conjunctivitis. In
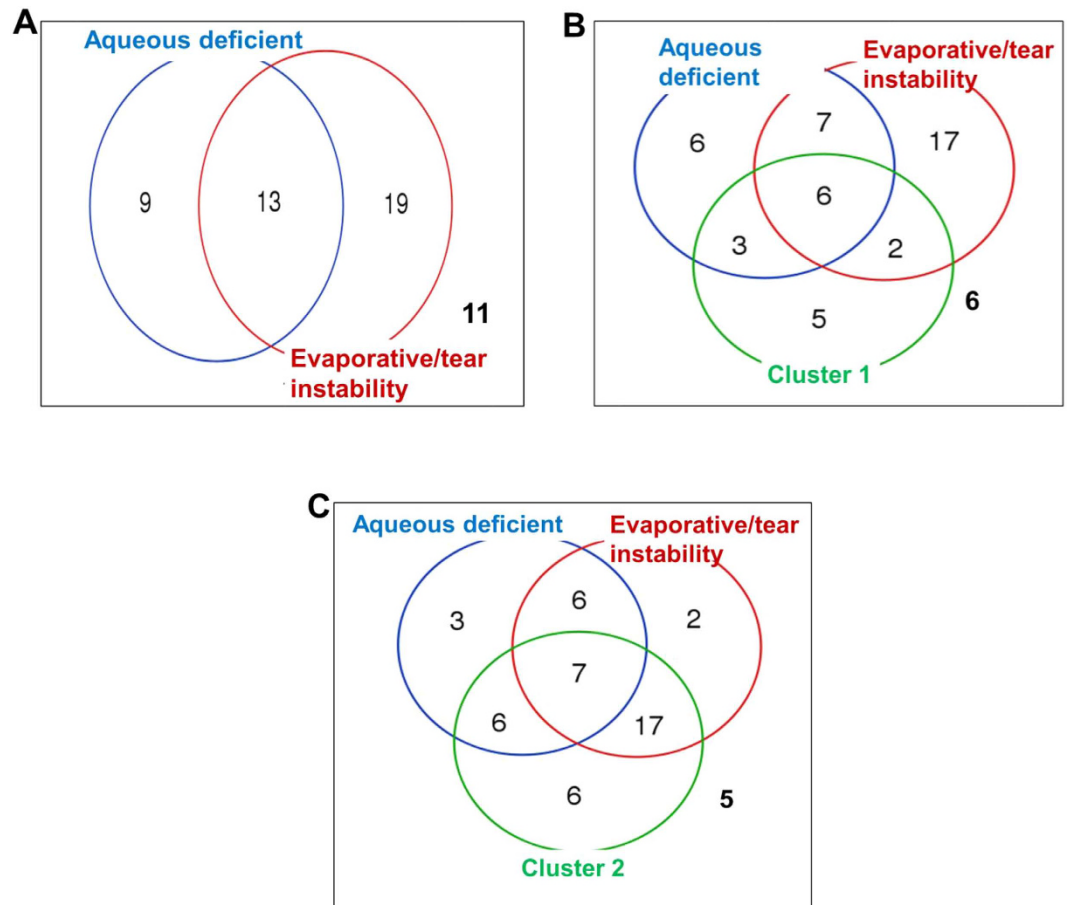
Figure 6. Venn Diagram analysis. (**A**) Proportion of DED patients (n = 52) with aqueous deficiency dry eye (Schirmer test <5 mm) or evaporative dry eye (NI-TBUT <6 s). (**B,C**) Proportion of Cluster-1 or Cluster-2 dry eye patients with aqueous deficiency dry eye or evaporative dry eye, respectively. The subject numbers analyzed for this diagram was 52. In all three panels, the numbers outside the circles are patients who did not qualify as aqueous, or evaporative or mixed. Venn diagram analysis was performed using online software at the following URL: http://bioinformatics.psb.ugent.be/webtools/Venn/.

experimental rodent DED, T cells are implicated in disease pathogenesis and adoptive transfer of pathogenic T cells is sufficient to impart DED in naïve recipients[23–27,32,36,37]. Although the T-cell immunosuppressant cyclosporine A is a cornerstone of DED therapy, the direct involvement of T cells in human DED is harder to demonstrate. Using immunohistochemistry on conjunctival biopsies, the involvement of CD4$^+$ and CD8$^+$ T cells in Sjogren and non-Sjogren DED patients has been reported[38,39]. More recently, impression cytology has been used to demonstrate the preponderance of mucosal-homing CD8$^+$ T$_{EM}$ cells in the conjunctiva of healthy individuals[40].

To determine if DED causes changes in the profile of recirculating and non-recirculating T cells, we used impression cytology and flow cytometry to study T cell subsets in the ocular surface of 52 patients with DED and 29 age- and gender-matched controls (Tables S1–S3). PCA revealed two distinct T-cell signatures (Fig. 7B,C), which we discovered to be associated with particular clinical features. Cluster-1 patients had increased conjunctival CD8$^+$ and CD4$^+$ CCR7$^+$ naïve and T$_{CM}$ T cells that may have been recruited to the ocular surface. Recruitment of CCR7$^+$ T cells to tissues is mediated by chemokines CCL19 and CCL21 that bind to the CCR7 receptor. Both chemokines are present in tear-duct associated lymphoid tissue, and expression of CCL21 is increased in inflamed cornea[41,42]. These chemokines may recruit naïve and T$_{CM}$ T cells to the ocular surface in Cluster-1 patients. These patients also had objectively increased OR (a measure of conjunctival hyperemia quantified by an Oculus Keratograph) compared to controls and Cluster-2 patients. The positive correlation between conjunctival naïve and T$_{CM}$ T cells and ocular redness suggests that the mechanisms underlying recruitment of CCR7$^+$ T cells to the ocular surface and induction of conjunctival hyperemia may be linked. NI-TBUT (measure of tear stability) was reduced in Cluster-1 patients compared to controls, but NI-TBUT was not correlated with the numbers of naïve and T$_{CM}$ T cells. We interpret this lack of correlation to mean that the recruitment of CCR7$^-$ T cells to the ocular surface is not related to the processes involved in tear evaporation, spreading and elasticity of tears.

Cluster-2 patients had similar absolute numbers of conjunctival CD3$^+$ T$_{EM}$ and T$_{EMRA}$ cells as controls, but the relative proportions of conjunctival CD8$^+$CD69$^+$CD103$^+$ T$_{EMRA}$-T$_{RM}$ and CD4$^+$CD69$^-$CD103$^+$T$_{EM}$-T$_{RCM}$ cells were increased compared to controls with a corresponding decrease in CD8$^+$CD69$^+$CD103$^-$ T$_{EMRA}$-T$_{RM}$
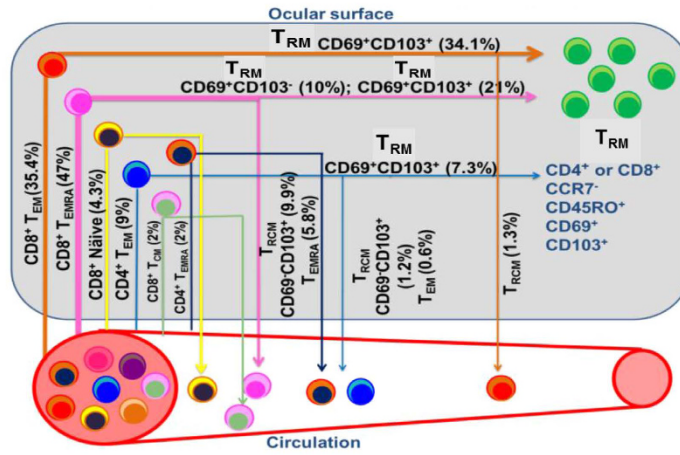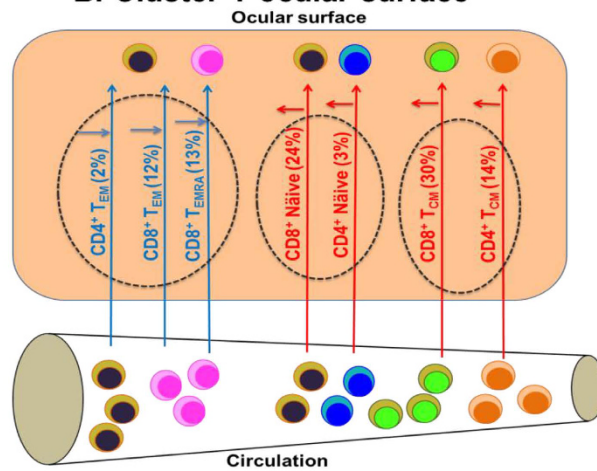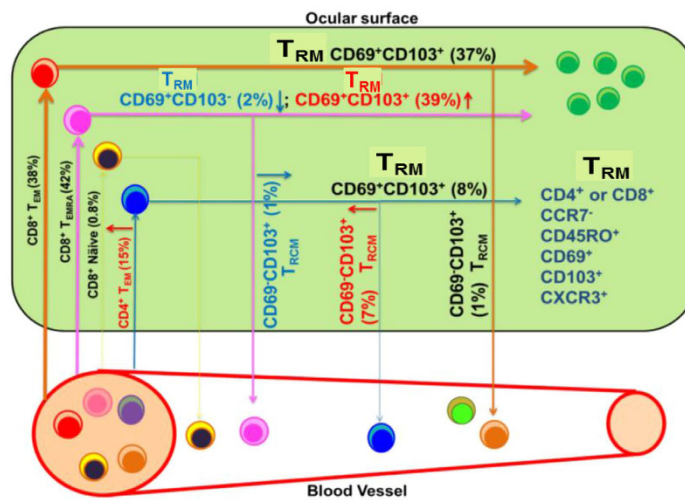
Figure 7. T cell subset patterns in the ocular surface in controls and cluster-1 and cluster -2 patients. (**A**) Schematic summarizing distribution of recirculating (naïve, T_{CM}, T_{EM}, T_{EMRA}, T_{RCM}) and non-recirculating (CD69+CD103− T_{RM}, CD69+CD103+ T_{RM}) T-subsets in the healthy human ocular surface. Numbers indicate the proportion of each subset within the CD3+ T cell pool. (**B**) Schematic summarizing distribution of conjunctival T-subsets in Cluster-1 patients. Numbers indicate the proportion of each subset within the CD3+ T cell pool. (**C**) Schematic summarizing distribution of conjunctival T-subsets in Cluster-2 patients. Numbers indicate the proportion of each subset within the CD3+ T cell pool.

and CD8$^+$CD69$^-$CD103$^+$ T$_{EMRA}$-T$_{RCM.}$ (*T cell signature-2*) (Fig. 7C). These patients exhibited reduced NI-TBUT compared to controls, with shorter NI-TBUT values correlating with higher proportions of conjunctival CD4$^+$ T$_{EM}$-T$_{RCM}$ and CD8$^+$ T$_{EMRA}$-T$_{RM}$s. The increased T$_{RM}$s and reduced NI-TBUT suggest that a chronic inflammatory process in Cluster-2 patients may have damaged elements on the ocular surface responsible for tear stability. In support, chronic DED in a rodent model is principally mediated by T$_{EM}$ Th17 cells[37].

Corticosteroids and/or cyclosporine are cornerstones of immunotherapy in DED[28–30]. Corticosteroids, while effective, raise intraocular pressure and cause glaucoma and cataracts with prolonged usage, while cyclosporine causes burning of the eyes[28–30]. Both drugs are broadly immunosuppressive. Novel immunotherapies that are more targeted are necessary. Since Cluster-1 patients exhibit increased CCR7$^+$ T cells on the ocular surface, inhibitors of CCR7 may have therapeutic benefit in these patients. Topical application of a blocking antibody against CCR7 has been reported to ameliorate ocular surface inflammation in an ovalbumin sensitization rodent model[42–44]. This therapeutic effect has been attributed to the suppression of CCR7$^+$ dendritic cells, but could also be due to suppression of CCR7$^+$ T cells. The K$_{Ca}$3.1 potassium channel is another target that could be engaged to preferentially suppress naïve and T$_{CM}$ T cells in Cluster-1 patients while sparing T$_{EM}$, T$_{EMRA}$ and T$_{RM}$ cells[45]. Senicapoc, a selective K$_{Ca}$3.1 blocker was shown to be safe in human trials for other indications[46], and could possibly be used topically for DED therapy. Since Cluster-2 patients have an increase in conjunctival CD8$^+$CD69$^+$CD103$^+$ T$_{EMRA}$-T$_{RM}$ and CD4$^+$CD69$^-$CD103$^+$T$_{EM}$-T$_{RCM}$ cell, drugs that preferentially target these subsets may have therapeutic benefit in these patients. The K$_v$1.3 potassium channel is widely regarded as a target for preferential suppression of CCR7$^-$ T$_{EM}$ and T$_{EMRA}$ cells[45], and a K$_v$1.3 inhibitor is in human trials as a therapeutic for autoimmune diseases[47]. Ocular formulations of K$_v$1.3 inhibitors may have used in the treatment of such patients. Alefacept, a drug that depletes effector memory T cells and evaluated in human clinical trials[48,49], may also be useful as an ocular formulation for Cluster-2 patients.

Our results show that the two conjunctival T-cell signatures of DED patients are unique classifiers. The proportion of patients with the evaporative/tear instability DED clinical sub-type are in a significantly higher in Cluster-2. Participants of clinical trials with DED could be stratified or selectively recruited based on T-cell signature, particularly if the treatment strategy selectively targets T-cell subsets. In medical centres which do not provide impression cytology and/or cytometric studies, documentation of OR, a non-invasive test, may provide a clue to the T-cell signature type in a DED patient. In a dry eye patient, elevation of OR suggests the T-cell signature of Cluster-1, and a normal OR suggests a Cluster-2 signature. Futures studies are required to determine if the two *T cell signatures* have differential prognosis or natural history in DED.

The strength of our study includes a uniform assessment of different kinds of patients with DED with objective and validated clinical tools. The limitation of our study is the lack of longitudinal data and the heterogeneity in terms of systemic treatment of these patients. It is extremely difficult to standardize treatment in a cross-sectional study, and would only be possible if assessment is performed as part of an interventional study where a uniform therapy can be started on freshly diagnosed patients. Another limitation is that we evaluated impression membranes instead of biopsies. Although these are relatively non-invasive, they may show a predisposition towards more superficial intraepithelial T cells as opposed to stromal cells and follicular T cells, and therefore do not represent the entire T cell population in the ocular surface mucosa. However, impression cytology is a standard procedure used in various studies of ocular surface disease[13,40].

In summary, the human ocular surface is protected by two subsets of T$_{RM}$s and four subsets of recirculating T cells, a profile resembling gastric mucosa more than skin, lung, intestine or cervix. We identify two clusters of DED that are distinguished by their immunological signatures and clinical tests. The two DED patient clusters may represent two distinct disease subsets with differing clinical outcomes, or they may represent interchangeable ends of an immune spectrum depending on whether inflammation is acute or chronic. Treatment follow-up studies are required to distinguish between these two possibilities. Our findings highlight the feasibility of stratifying DED into distinct sub-types that will allow assessment of treatment responsiveness, clinical outcomes, disease evolution, and prognosis. Our findings also open the door to novel sub-type-targeted therapies, which will complement current therapies.

Materials and Methods

Ethics. Human ocular samples were collected from Singapore National Eye Centre. The SingHealth Centralized Institutional Review Board and the Nanyang Technological University Institutional Review Board, Singapore approved all studies described here. Tenets of the Declaration of Helsinki were adhered to. All patients who met the eligibility criteria at the dry eye clinic in Singapore National Eye Centre went through study briefing and were invited for screening. Written informed consent was obtained from enrolled participants by the clinical trial coordinator. The study was registered at the clinicaltrials.gov database (Singapore National Eye Centre). Impression samples were collected few hours after medical tests were performed.

Non-invasive tear breakup time (NI-TBUT). We used the Oculus K5M to measure NI-TBUT[50,51]. Using infrared monitoring of the tear film, the Oculus algorithm documents the time and site of tear film breakup[34]. NI-TBUT value <10 secs was considered indicative of dry eye disease symptoms.

Ocular redness. We used the Oculus K5M to objectively assess bulbar and peri-limbal redness of the eye. We took a photo of the ocular surface under white light with the Oculus camera and analyzed by comparing with a standard grading system (JENVIS) ranging from 0 (no redness) to 4.0 (maximum). The analysis also provided separate measures of redness of the temporal and nasal conjunctiva[33,34]. The following variables were used in the analysis: temporal bulbar OR, nasal bulbar OR, bulbar OR, limbal OR, total conjunctival OR. We used average OR values of the two eyes, as well as worse eye OR between the 2 eyes for analyses. These different ways of

computing OR were used in order to ensure robustness of the findings, as there is no single universal parameter or threshold that is currently agreed upon.

Schirmer's Test.   We measured baseline tear secretion using the Schirmer's Test as described[52]. A Schirmer's value <5 mm was considered indicative of tear hypo-secretion.

SPEED questionnaire.   We used the Standard Patient Evaluation of Eye Dryness (SPEED) questionnaire to assess dryness, irritation, burning and fatigue. All patients with DED had high SPEED scores[53].

Impression cytology.   Impression samples were collected from nasal and bulbar portions of the eye by EyePrim technology after performing clinical tests on the subjects. Cells were isolated after collection by continuous scraping with a pipette tip. After scraping, cells were washed two times with flow cytometry staining buffer (PBS with 0.05% BSA).

Flow cytometry.   Samples isolated by impression cytology were incubated with fluorescent antibodies for 20–30 min and washed twice with staining buffer before measurement with the BD FACSVerse flow cytometer (BD Bioscience, San Jose, CA). All antibodies were purchased from BD Bioscience: CD3 brilliant violet 510 (BV510) (UCHT1), CD4 allophycocyanine-H7 (APC-H7) (SK3), CD8-fluorescein isothiocyanate (FITC) (RPA-T8), CD197/ CCR7 phycoerythrin (PE) (3D12), CD45RO phycoerythrin-cyanine7 (PE-Cy7) (UCHL1), Cell viability solution (7-aminoactinomycin D, 7-AAD), CD69 APC (FN50), CD103 BV421 (Ber-ACT8).

Statistical analysis.   Graphs were generated and statistical analyses were performed in GraphPad Prism 6.0 (GraphPad, La Jolla, CA). Statistical tests were evaluated using Mann-Whitney unpaired t-test and all data are expressed as mean $\pm$ SEM if not stated otherwise. $*P < 0.05$; $**P < 0.01$; $***P < 0.001$. Venn Diagram analysis was performed using online software with the following url link: http://bioinformatics.psb.ugent.be/webtools/Venn/.

References

1. Sallusto, F., Geginat, J. & Lanzavecchia, A. Central memory and effector memory T cell subsets: function, generation, and maintenance. Annual review of immunology **22,** 745–763 (2004).
2. Thome, J. J. & Farber, D. L. Emerging concepts in tissue-resident T cells: lessons from humans. *Trends Immunol* **36,** 428–435 (2015).
3. Park, C. O. & Kupper, T. S. The emerging role of resident memory T cells in protective immunity and inflammatory disease. *Nature Medicine* **21,** 688–697 (2015).
4. Watanabe, R. *et al.* Human skin is protected by four functionally and phenotypically discrete populations of resident and recirculating memory T cells. Sci Transl Med **7,** 279ra239 (2015).
5. Clark, R. A. Resident memory T cells in human health and disease. Sci Transl Med **7,** *269rv261* (2015).
6. Purwar, R. *et al.* Resident memory T cells (T_{RM}) are abundant in human lung: diversity, function, and antigen specificity. *PLoS One* **6,** e16245 (2011).
7. Teijaro, J. R. *et al.* Cutting edge: Tissue-retentive lung memory CD4 T cells mediate optimal protection to respiratory virus infection. *Journal of immunology* **187,** 5510–5514 (2011).
8. Sathaliyawala, T. *et al.* Distribution and compartmentalization of human circulating and tissue-resident memory T cell subsets. *Immunity* **38,** 187–197 (2013).
9. Turner, D. L. *et al.* Lung niches for the generation and maintenance of tissue-resident memory T cells. *Mucosal Immunol* **7,** 501–510 (2014).
10. Booth, J. S. *et al.* Characterization and functional properties of gastric tissue-resident memory T cells from children, adults, and the elderly. *Frontiers in immunology* **5,** 294 (2014).
11. Mueller S. N. & Mackay L. K. Tissue-resident memory T cells: local specialists in immune defence. *Nat Rev Immunol* **16,** 79–89 (2016).
12. Leong, Y. Y. & Tong, L. Barrier function in the ocular surface: from conventional paradigms to new opportunities. *The ocular surface* **13,** 103–109 (2015).
13. Williams, G. P. *et al.* The dominant human conjunctival epithelial CD8alphabeta + T cell population is maintained with age but the number of CD4^{+} T cells increases. *Age (Dordr)* **34,** 1517–1528 (2012).
14. Knop, E. & Knop, N. The role of eye-associated lymphoid tissue in corneal immune protection. *Journal of Anatomy* **206,** 271–285 (2005).
15. The epidemiology of dry eye disease: report of the Epidemiology Subcommittee of the International Dry Eye WorkShop. *The ocular surface* **5,** 93–107 (2007).
16. Paulsen, A. J. *et al.* Dry eye in the beaver dam offspring study: prevalence, risk factors, and health-related quality of life. *American Journal of Ophthalmology* **157,** 799–806 (2014).
17. Lin, P. Y. *et al.* Prevalence of dry eye among an elderly Chinese population in Taiwan: the Shihpai Eye Study. *Ophthalmology* **110,** 1096–1101 (2003).
18. Dalzell, M. D. Dry eye: prevalence, utilization, and economic implications. *Manag Care* **12,** 9–13 (2003).
19. Yu, J., Asche, C. V. & Fairchild, C. J. The economic burden of dry eye disease in the United States: a decision tree analysis. *Cornea* **30,** 379–387 (2011).
20. Uchino, M. & Schaumberg, D. A. Dry Eye Disease: Impact on Quality of Life and Vision. *Curr* Ophthalmol Rep **1,** 51–57 (2013)
21. The definition and classification of dry eye disease: report of the Definition and Classification Subcommittee of the International Dry Eye Work Shop (2007). *The Ocular Surface* **5,** 75–92 (2007).
22. Saboo, U. S., Amparo, F., Abud, T. B., Schaumberg, D. A. & Dana, R. Vision-Related Quality of Life in Patients with Ocular Graft-versus-Host Disease. *Ophthalmology* **122,** 1669–1674 (2015).
23. Li, H., Dai, M. & Zhuang, Y. A. T cell intrinsic role of Id3 in a mouse model for primary Sjogren's syndrome. *Immunity* **21,** 551–560 (2004).
24. Shen, L. *et al.* Development of autoimmunity in IL-14alpha-transgenic mice. *Journal of Immunology* **177,** 5676–5686 (2006).
25. Jiang, G. *et al.* A new model of experimental autoimmune keratoconjunctivitis sicca (KCS) induced in Lewis rat by the autoantigen Klk1b22. *Investigative Ophthalmology & Visual Science* **50,** 2245–2254 (2009).
26. Lieberman, S. M., Kreiger, P. A. & Koretzky, G. A. Reversible lacrimal gland-protective regulatory T-cell dysfunction underlies male-specific autoimmune dacryoadenitis in the non-obese diabetic mouse model of Sjogren syndrome. *Immunology* **145,** 232–241 (2015).

27. Yaciuk, J. C. *et al.* Defective selection of thymic regulatory T cells accompanies autoimmunity and pulmonary infiltrates in Tcra-deficient mice double transgenic for human La/Sjogren's syndrome-B and human La-specific TCR. *Journal of Immunology* **194,** 1514–1522 (2015).

28. Tong, L., Thumboo, J., Tan, Y. K., Wong, T. Y. & Albani, S. The eye: a window of opportunity in rheumatoid arthritis? *Nat Rev Rheumatol* **10,** 552–560 (2014).

29. Coursey, T. G. & de Paiva, C. S. Managing Sjogren's Syndrome and non-Sjogren Syndrome dry eye with anti-inflammatory therapy. *Clin Ophthalmol* **8,** 1447–1458 (2014).

30. Novack, G. D. Pharmacologic treatments for dry eye: a worthwhile investment? *Cornea*, 4–5 (2002).

31. Bromley, S. K., Yan, S., Tomura, M., Kanagawa, O. & Luster, A. D. Recirculating memory T cells are a unique subset of CD4+ T cells with a distinct phenotype and migratory pattern. *Journal of Immunology* **190,** 970–976 (2013).

32. Coursey, T. G., Gandhi, N. B., Volpe, E. A., Pflugfelder, S. C. & de Paiva, C. S. Chemokine receptors CCR6 and CXCR3 are necessary for CD4+ T cell mediated ocular surface disease in experimental dry eye disease. *PLoS One.* **8,** e78508 (2013).

33. Best, N., Drury, L. & Wolffsohn, J. S. Clinical evaluation of the Oculus Keratograph. *Cont Lens Anterior Eye* **35,** 171–174 (2012).

34. Downie, L. E., Keller, P. R. & Vingrys, A. J. Assessing ocular bulbar redness: a comparison of methods. *Ophthalmic Physiol Opt* **36,** 132–139 (2016).

35. Amparo, F., Wang, H., Emami-Naeini, P., Karimian, P. & Dana, R. The Ocular Redness Index: a novel automated method for measuring ocular injection. *Investigative Ophthalmology & Visual Science* **54,** 4821–4826 (2013).

36. Niederkorn J. Y., Stern M. E., Pflugfelder S. C., De Paiva C. S., Corrales R. M., Gao, J. & Siemasko K. Desiccating stress induces T cell-mediated Sjögren's Syndrome-like lacrimal keratoconjunctivitis. *J Immunol.* **176,** 3950–3957 (2006).

37. Chen, Y., Chauhan, S. K., Lee, H. S., Saban, D. R. & Dana, R. Chronic dry eye disease is principally mediated by effector memory Th17 cells. *Mucosal Immunol.* **7,** 38–45 (2014).

38. Knop N. & Knop E. Regulation of the inflammatory component in chronic dry eye disease by the eye-associated lymphoid tissue (EALT). *Dev Ophthalmol.* **45,** 23–39 (2010).

39. Stern, M. E. *et al.* Conjunctival T-cell subpopulations in Sjögren's and non-Sjögren's patients with dry eye. *Invest Ophthalmol Vis Sci.* **43,** 2609–2614 (2002).

40. Williams, G. P., Pachnio, A., Long, H. M., Rauz, S. & Curnow, S. J. Cytokine production and antigen recognition by human mucosal homing conjunctival effector memory CD8+ T cells. *Invest Ophthalmol Vis Sci.* **55,** 8523–30 (2014).

41. Nagatake, T. *et al.* Id2-, RORgammat-, and LTbetaR-independent initiation of lymphoid organogenesis in ocular immunity. *The Journal of Experimental Medicine* **206,** 2351–2364, (2009).

42. Jin, Y., Shen, L., Chong, E. M. Hamrah, P., Zhang, Q., Chen, L. & Dana, M. R. The chemokine receptor CCR7 mediates corneal antigen-presenting cell trafficking. *Mol Vis* **13,** 626–634 (2007).

43. Kodati, S. *et al.* CCR7 is critical for the induction and maintenance of Th17 immunity in dry eye disease. *Investigative Ophthalmology & Visual Science* **55,** 5871–5877 (2014).

44. Saban, D. R. The chemokine receptor CCR7 expressed by dendritic cells: a key player in corneal and ocular surface inflammation. *The Ocular Surface* **12,** 87–99 (2014).

45. Cahalan, M. D. & Chandy, K. G. The functional network of ion channels in T lymphocytes. *Immunol Rev* **231,** 59–87 (2009).

46. Ataga K. I., Reid M., Ballas S. K., Yasin Z., Bigelow C., James L. S., Smith W. R., Galacteros F., Kutlar A., Hull J. H. & Stocker J. W.; ICA-17043-10 Study Investigators. Improvements in haemolysis and indicators of erythrocyte survival do not correlate with acute vaso-occlusive crises in patients with sickle cell disease: a phase III randomized, placebo-controlled, double-blind study of the Gardos channel blocker senicapoc (ICA-17043). *Br J Haematol.* **153,** 92–104 (2011).

47. Chandy, K. G. & Norton, R. S. Immunology: Channelling potassium to fight cancer. *Nature.* **537,** 497–499 (2016).

48. Ellis, C. N. & Krueger, G. G. & Alefacept Clinical Study Group. Treatment of chronic plaque psoriasis by selective targeting of memory effector T lymphocytes. *N Engl J Med.* **345,** 248–255 (2001).

49. Rigby, M. R. *et al.* Alefacept provides sustained clinical and immunological effects in new-onset type 1 diabetes patients. *J Clin Invest.* **125,** 3285–3296 (2015).

50. Jiang, Y., Ye, H., Xu, J. & Lu, Y. Noninvasive Keratograph assessment of tear film break-up time and location in patients with age-related cataracts and dry eye syndrome. *J Int Med Res* **42,** 494–502 (2014).

51. Hong, J. *et al.* Evaluation of age-related changes in noninvasive tear breakup time. *Optom Vis Sci* **91,** 150–155 (2014).

52. Shapiro, A. & Merin, S. Schirmer test and break-up time of tear film in normal subjects. *American Journal of Ophthalmology* **88,** 752–757 (1979).

53. Finis, D. *et al.* Comparison of the OSDI and SPEED questionnaires for the evaluation of dry eye disease in clinical routine. *Ophthalmologe* **111,** 1050–1056 (2014).

Acknowledgements

Author Contributions

T.B., L.T. and K.G.C. concieved and designed experiments. T.B., R.L. and A.H. performed the experiments; T.B., R.L., L.T. and K.G.C. analyzed the data; T.B. prepared figures; and K.G.C., T.B. and L.T.wrote the manuscript. All authors reviewed the manuscript.

Additional Information

Supplementary information accompanies this paper at http://www.nature.com/srep

Competing Interests: The authors declare no competing financial interests.

How to cite this article: Bose, T. *et al.* Tissue resident memory T cells in the human conjunctiva and immune signatures in human dry eye disease. *Sci. Rep.* **7,** 45312; doi: 10.1038/srep45312 (2017).

Publisher's note: Springer Nature remains neutral with regard to jurisdictional claims in published maps and institutional affiliations.